




Spatiotemporal metabolic dynamics of the photosensitizer talaporfin sodium in carcinoma and sarcoma

Takuma Saito^{1,2} | Tomohide Tsukahara¹  | Takeshi Suzuki³ | Iyori Nojima⁴ | Hiroki Tadano^{1,5} | Noriko Kawai^{1,6} | Terufumi Kubo¹  | Yoshihiko Hirohashi¹  | Takayuki Kanaseki¹ | Toshihiko Torigoe¹ | Liming Li²

¹Department of Pathology, Sapporo Medical University School of Medicine, Sapporo, Japan

²Graduate School of Photonic Science, Chitose Institute for Science and Technology, Sapporo, Japan

³Department of Biology, Sapporo Medical University School of Medicine, Sapporo, Japan

⁴Division of Cell Bank, Biomedical Research, Education and Instrumentation Center, Sapporo Medical University School of Medicine, Sapporo, Japan

⁵Division of Internal Medicine, Sapporo Self-Defense Forces Hospital, Sapporo, Japan

⁶Department of Gastroenterological Surgery II, Hokkaido University Graduate School of Medicine, Sapporo, Japan

Correspondence

Tomohide Tsukahara, Department of Pathology, Sapporo Medical University School of Medicine, South-1, West-17, Chouku, Sapporo, Hokkaido 060-8556, Japan.
Email: tsukahara@sapmed.ac.jp

Funding information

the Takeda Science Foundation, Grant/Award Number: 2018-Kenkyu-Shorei Keizoku; the Research Grant of Princess Takamatsu Cancer Research Fund, Grant/Award Number: 19-25125; Japan Society for the Promotion of Science, Grant/Award Number: 17H01540, 20H03807 and 25462344

Abstract

Photodynamic therapy (PDT) using the photosensitizer talaporfin sodium (talaporfin) is a new mode of treatment for cancer. However, the metabolic mechanism of talaporfin has not been clarified. Thus, we investigated the uptake, transportation, and elimination mechanisms of talaporfin in carcinoma and sarcoma. The results showed that talaporfin co-localized in early endosomes and lysosomes. Talaporfin uptake was via clathrin- and caveolae-dependent endocytosis and a high amount of intracellular ATP was essential. Inhibition of lysosomal enzymes maintained intracellular talaporfin levels. Inhibition of K-Ras signaling reduced talaporfin uptake in carcinoma and sarcoma cell lines. Talaporfin was taken up by clathrin- and caveolae-dependent endocytosis, translocated from early endosomes to lysosomes, and finally degraded by lysosomes. We also demonstrated that ATP is essential for the uptake of talaporfin and that activation of K-Ras is involved as a regulatory mechanism. These results provide new insights into the metabolism of talaporfin in cancer cells for the enhancement of PDT for carcinoma and sarcoma.

KEYWORDS

ATP, endocytosis, K-RAS, lysosome, talaporfin sodium

1 | INTRODUCTION

Photodynamic diagnosis (PDD) and photodynamic therapy (PDT) using talaporfin sodium (talaporfin) as a photosensitizer has attracted attention as a new mode of cancer treatment. PDD is a diagnostic method

that detects fluorescence emitted from tumor tissue, and PDT is a therapeutic method that kills cancer cells with reactive oxygen species (ROS) generated from photosensitive substances.¹ Talaporfin, which is derived from chlorophyll and L-aspartic acid, is a second-generation photosensitizer that improves the efficiency of ROS generation and

This is an open access article under the terms of the Creative Commons Attribution-NonCommercial License, which permits use, distribution and reproduction in any medium, provided the original work is properly cited and is not used for commercial purposes.

© 2020 The Authors. *Cancer Science* published by John Wiley & Sons Australia, Ltd on behalf of Japanese Cancer Association.

reduces side-effects compared with first-generation photosensitizers such as hematoporphyrin derivatives.² The half-life of talaporfin is 138 hours and that of the first-generation photosensitizer porfimer is 250 hours. The fact that talaporfin is eliminated faster might contribute to reduced side-effects and accelerate the timing of laser irradiation. Laser irradiation is carried out at 4-6 hours after injection of talaporfin in patients with lung and esophageal cancer, which is much shorter than the 48-72 hours patients must wait when porfimer is used. Moreover, cell death after PDT could induce anti-tumor immune responses through the activation of immune cells, cytokine release, and CD8+ T cell infiltration into the tumor, followed by the formation of immunological memory.^{3,4} Talaporfin has been used in PDT for some cancers, but its specific uptake and discharge mechanisms for cancer cells have not been clarified.

Endocytosis and transporters have been confirmed as the mechanisms of drug uptake and elimination by cells. Endocytosis regulates nutrient uptake, the cell expression level of surface receptors, plasma membrane turnover and cellular signaling, and is required for cell spreading, polarization and migration.⁵ In addition, endocytosis also affects drug resistance in cancer cells.⁶ Transporters function in the transportation and discharge of drugs and toxins that affect the growth, survival, and migration of cancer cells.⁷ A previous study suggested that the potential uptake of talaporfin is mediated by endocytosis;⁸ however, the detailed mechanisms have not been clarified.

In the present study, we investigated the mechanisms of uptake and elimination of talaporfin in carcinoma and sarcoma cells. We show that the uptake of talaporfin was mediated by endocytosis via clathrin and caveolae and transferred from early endosomes to lysosomes, followed by degradation in the lysosomes. Moreover, in the uptake of talaporfin, a high amount of ATP was essential as was to a lesser degree activation of the Ras signaling pathway.

2 | MATERIALS AND METHODS

This study was performed in accordance with the guidelines established by the Declaration of Helsinki and was approved by the Ethics Committee of Sapporo Medical University. The healthy donors provided informed consent for the use of blood samples in our research.

2.1 | Cell lines and culture

The cell lines used in this study are shown in Table S1. Osteosarcoma cell lines OS2000 and OS13 and the bone

malignant fibrous histiocytoma cell line MFH03 were established in our laboratory.⁹⁻¹¹ The other cell lines were purchased from the Japanese Collection of Research Bioresources Cell Bank (Tokyo, Japan) and the ATCC (Manassas, VA). All cell lines were cultured in a 5% CO₂ incubator.

2.2 | Temporal analysis of talaporfin uptake

Each cell line was suspended at 1.0×10^6 cells/mL in a serum-free DMEM, RPMI-1640, IMDM, HamF12 or AIM-V. Talaporfin sodium (Meiji Seika Co. Ltd, Tokyo, Japan) was added to a final concentration of 30 µg/mL and cultured at 37°C for 1-4 hours. After incubation, the medium was removed, washed three times with PBS, fixed with 0.5% formalin, and analyzed with a BD FACSCanto II flow cytometer (Becton-Dickinson, Mountain View, CA). For the detection of talaporfin fluorescence, a long-pass filter of 655 nm/670 nm was used for 488 nm excitation light. Unstained cells were used as a negative control.

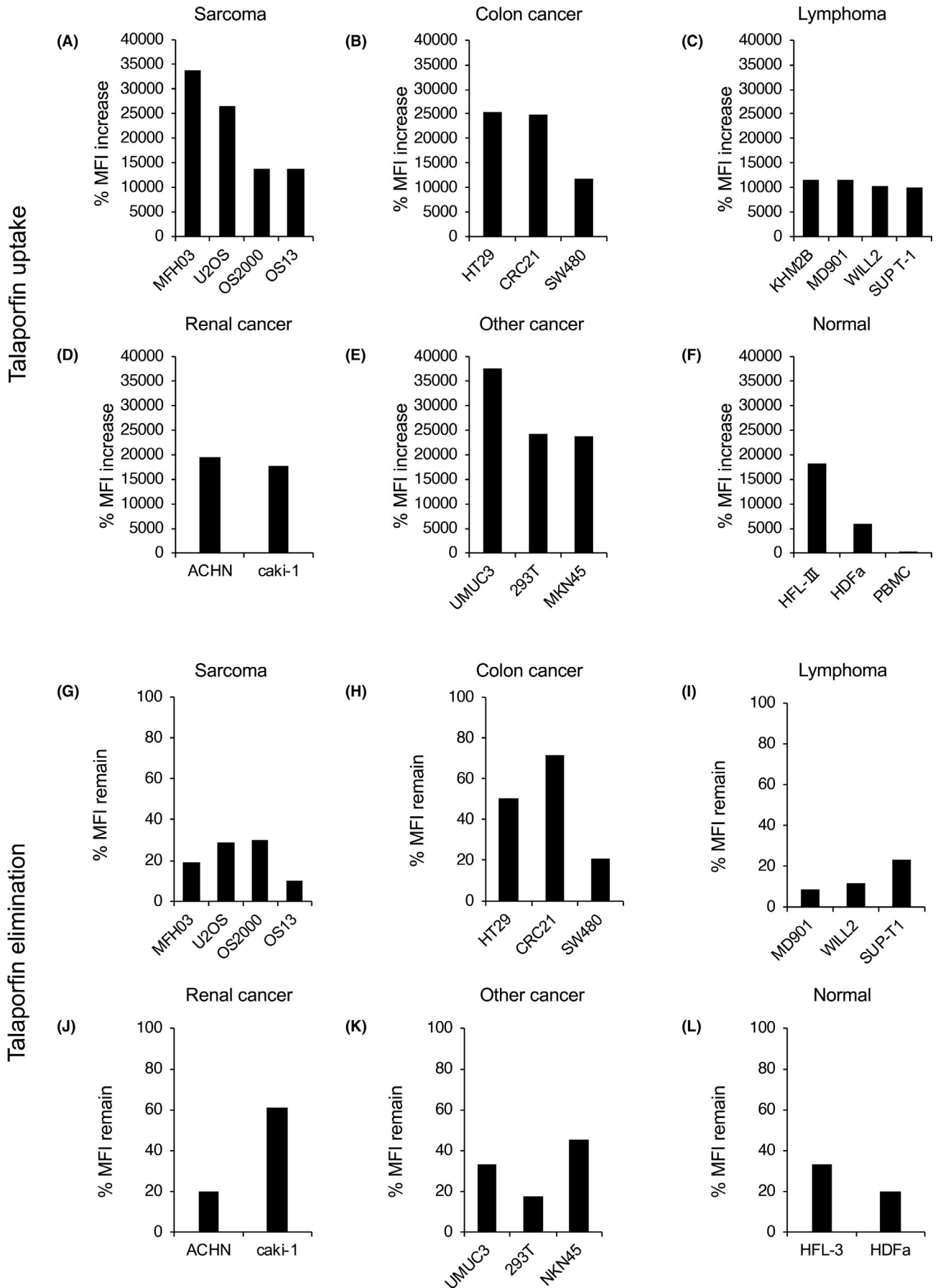
2.3 | Analysis of hourly excretion of talaporfin in different cells

Each cell line was seeded in a T25 cell culture flask (Corning Inc., Corning, NY) using serum-free DMEM, RPMI-1640, IMDM, HamF12 or AIM-V 24 hours before the experiment and cultured to approximately 80% confluence. The medium was removed, washed once with PBS, and cultured in the medium supplemented with talaporfin for 1 hour at 37°C. After incubation, the medium was replaced with 5 mL fresh medium, followed by culture at 37°C for 1-24 hours. The cells were washed three times with PBS, fixed with 0.5% formalin and analyzed by flow cytometer.

2.4 | Analysis of intracellular dynamics of talaporfin localization

Cells were seeded on a 35-mm glass base dish (Iwaki Glass, Tokyo, Japan) 24 hours before the experiment and cultured to 1×10^5 cells/well. CellLight lysosomes-GFP (Thermo Fisher Scientific, Waltham, MA) or CellLight Early Endosomes-GFP (Thermo Fisher Scientific) was added at 10-50 particles per cell (PPC) and incubated overnight. After incubation, the medium was replaced with fresh medium supplemented with talaporfin at concentrations of 30 µg/mL, 60 µg/mL, and 100 µg/mL. The cells were washed three times every

FIGURE 1 Variability in the uptake and elimination of talaporfin in various cancer and normal cell lines. (A-F) Change of mean fluorescence intensity of indicated cell lines after incubation with talaporfin (30 µg/mL) for 4 h. (G-L) Change of mean fluorescence intensity of indicated cell lines after 1 h incubation with talaporfin following removal of extracellular talaporfin after 24 h. Mean fluorescence intensity increase (%MFI increase) (A-F) was calculated using the following formula: %MFI increase = [(MFI of talaporfin-treated) - (MFI of non-treated)]/(MFI of non-treated) × 100. Mean fluorescence intensity remaining (%MFI remain) (G-L) was calculated using the following formula: %MFI remain = [(MFI after talaporfin-eliminated)/(MFI of talaporfin-pretreated)] × 100. All experiments were repeated three times



20 minutes, fixed with 0.5% formalin, and analyzed using a confocal laser scanning microscope (ELYRA PS.1/LSM 780; Carl Zeiss, Oberkochen, Germany).

2.5 | Blocking assay of endocytosis

Cells were suspended in DMEM or IMDM at 1.0×10^6 cells/mL in 1.5 mL microtubes. After the uptake of talaporfin, the following endocytosis inhibitors were added: 2-deoxyglucose (2-DG; Sigma-Aldrich, St Louis, MO) at a concentration of 50 mmol/L, sodium azide (0.1% w/v; Kanto Chemical, Tokyo, Japan), methyl- β -cyclodextrin (5 mmol/L; Wako, Osaka, Japan), genistein (0.1 mmol/L; Wako), sucrose (0.45 M; Wako), chlorpromazine hydrochloride (20 mmol/L; Tokyo Chemical, Tokyo, Japan), cytochalasin β (1 mmol/L; Wako) and colchicine (1 mmol/L; Wako). After culture at 37°C for 30 minutes, the cells were chilled on ice for 30 minutes, washed three times with PBS, fixed with 0.5% formalin and analyzed by flow cytometry. For the inhibition of clathrin-dependent endocytosis, Pitstop 2 (ab120687; Abcam, Cambridge, UK) was added to the serum-free DMEM or IMDM to a final concentration of 25 μ mol/L, and the cells were cultured at 37°C for 1 hour. Talaporfin was subsequently added to the cells to a final concentration of 30 μ g/mL and the cells were washed three times with PBS, fixed with 0.5% formalin, and analyzed by flow cytometry.

2.6 | Blocking assay of lysosomal degradation of talaporfin

Cells were seeded in a 6-well plate at 3×10^5 cells/mL. After 24 hours, talaporfin was added to IMDM at concentrations of 30 μ g/mL or 100 μ g/mL, and cells were cultured for 24 or 1 hour at 37°C. After staining with talaporfin, the cells were washed once with PBS and cultured in IMDM containing chloroquine (CQ; 12.5 μ g/mL, 25 μ g/mL) or NH_4Cl (5 mg/mL, 10 mg/mL) for 48 hours at 37°C. Cells were then washed three times with PBS, fixed with 0.5% formalin, and analyzed by flow cytometry.

2.7 | Measurement of ATP production

Cellular ATP levels were measured using Cellno ATP assay kit (Toyo B-Net Co., Ltd, Tokyo, Japan) according to the manufacturer's protocol. Cells were cultured in 96-well flat plates with DMEM or IMDM for 30 minutes. After incubation, luminescence intensity was measured using an Infinite M1000 Pro plate reader (Tecan, Männedorf, Switzerland).

2.8 | Inhibition assay of Ras signaling pathway

A549 and MIA PaCa2 cells with K-Ras mutation were used.^{12,13} HDFa cells, the keratinocyte cell line, were used as the control. Cells were

seeded in a 6-well plate at 1×10^6 cells/well and preincubated for 24 hours. The following Ras signaling pathway inhibitors were used: wortmannin (at concentrations of 2 nmol/L, 20 nmol/L, 200 nmol/L), ZSTK474 (at concentrations of 0.01 μ mol/L, 0.1 μ mol/L, 1 μ mol/L), sorafenib (at concentrations of 0.5 μ mol/L, 5 μ mol/L, 50 μ mol/L), and trametinib (at concentrations of 0.1 mmol/L, 1 mmol/L, 10 mmol/L). The inhibitors were added and cultured for 1 hour. The medium was removed, washed once with $1 \times$ PBS, and serum-free DMEM containing a final concentration of 30 μ g/mL talaporfin was added. The cells were washed three times with PBS, fixed with 0.5% formalin, and analyzed by flow cytometry.

2.9 | RT-PCR

Total RNA samples were extracted using TRIzol (Qiagen, Germantown, MD), and cDNA samples were synthesized with 2 μ g total RNA using Superscript III Reverse Transcriptase (Invitrogen, Eugene, OR) in accordance with the manufacturer's protocol. PCR was carried out using Taq DNA polymerase (Qiagen) under the following conditions: initial denaturation for 2 minutes at 94°C, followed by 35 cycles of denaturation for 15 s at 94°C, annealing for 30 s at 56°C, elongation for 30 s at 72°C, and a final elongation step for 5 minutes at 72°C. The primers used in experiments are summarized in Table S2.

3 | RESULTS

3.1 | Intracellular talaporfin levels increased after incubation with talaporfin and decreased after removal of extracellular talaporfin in various carcinoma and sarcoma cells

We investigated whether there was a difference in intracellular levels of talaporfin after incubation with talaporfin and after removal of extracellular talaporfin among various cell lines. Intracellular talaporfin levels increased in all cell lines at various levels except for PBMC, as shown in Figure 1 and Table S3. Subsequently, intracellular talaporfin also decreased at various levels 24 hours after removal of extracellular talaporfin in all cell lines (Table S3).

3.2 | Incorporated talaporfin translocates from early endosomes to lysosomes

To assess the mechanisms of drug uptake and elimination, we first focused on ATP-binding cassette (ABC) transporters involved in cancer multidrug resistance. However, we could not identify the specific expression of ABC transporters (Figure S1).

Next, we focused on endocytosis as a candidate mechanism of talaporfin metabolism. We analyzed the colocalization of talaporfin, with Rab5a, the lysosomal antigen LAMP1, and mitochondria in the

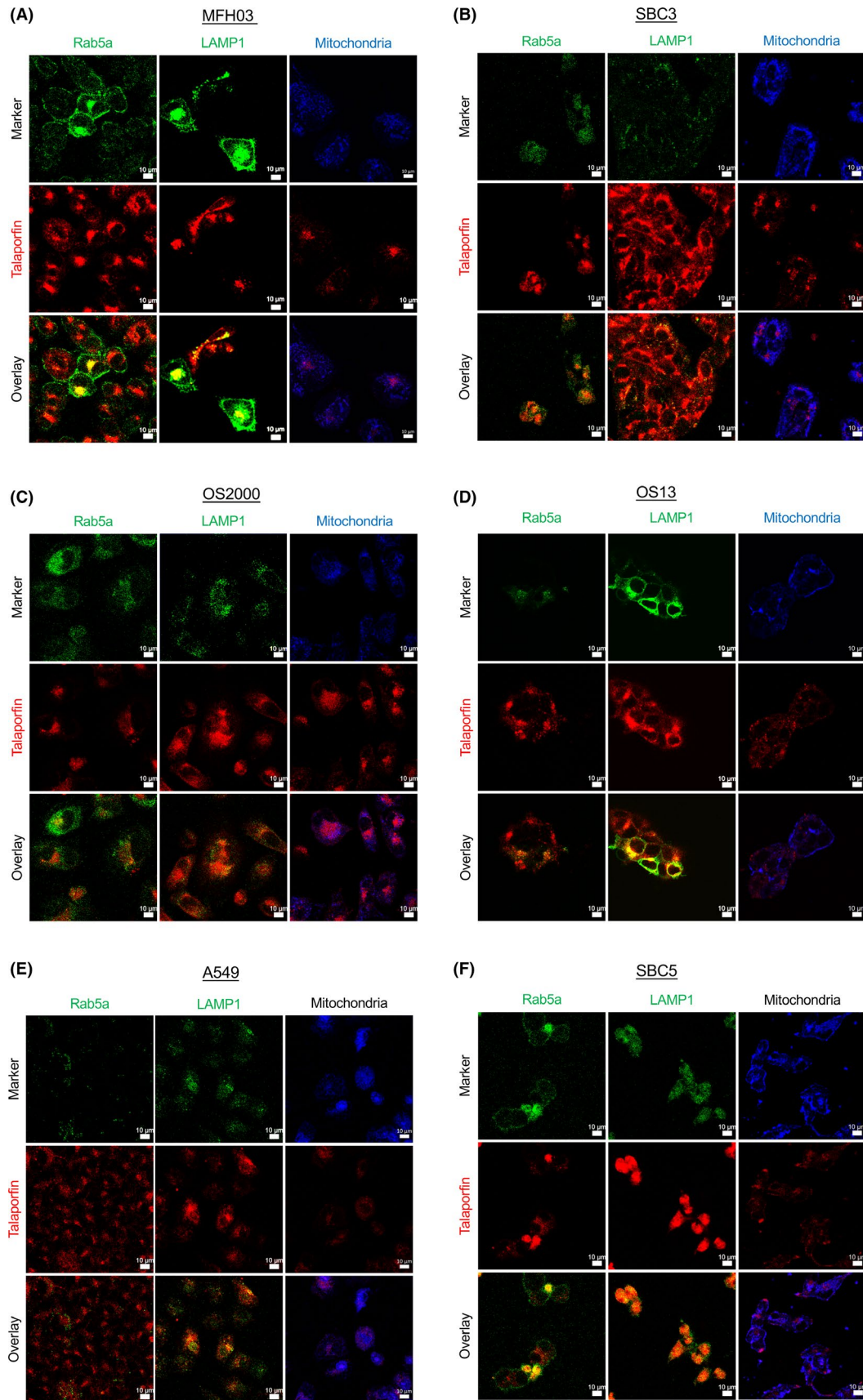


FIGURE 2 Intracellular talaporfin was colocalized with early endosomes and lysosomes but not with mitochondria. Fluorescence microscopy images of Rab5a, lysosomal membrane protein 1 (LAMP1), mitochondria, and talaporfin in sarcoma cell line (A, C, D) and lung cancer cell line (B, E, F) are shown in the indicated colours. Bar = 10 µm

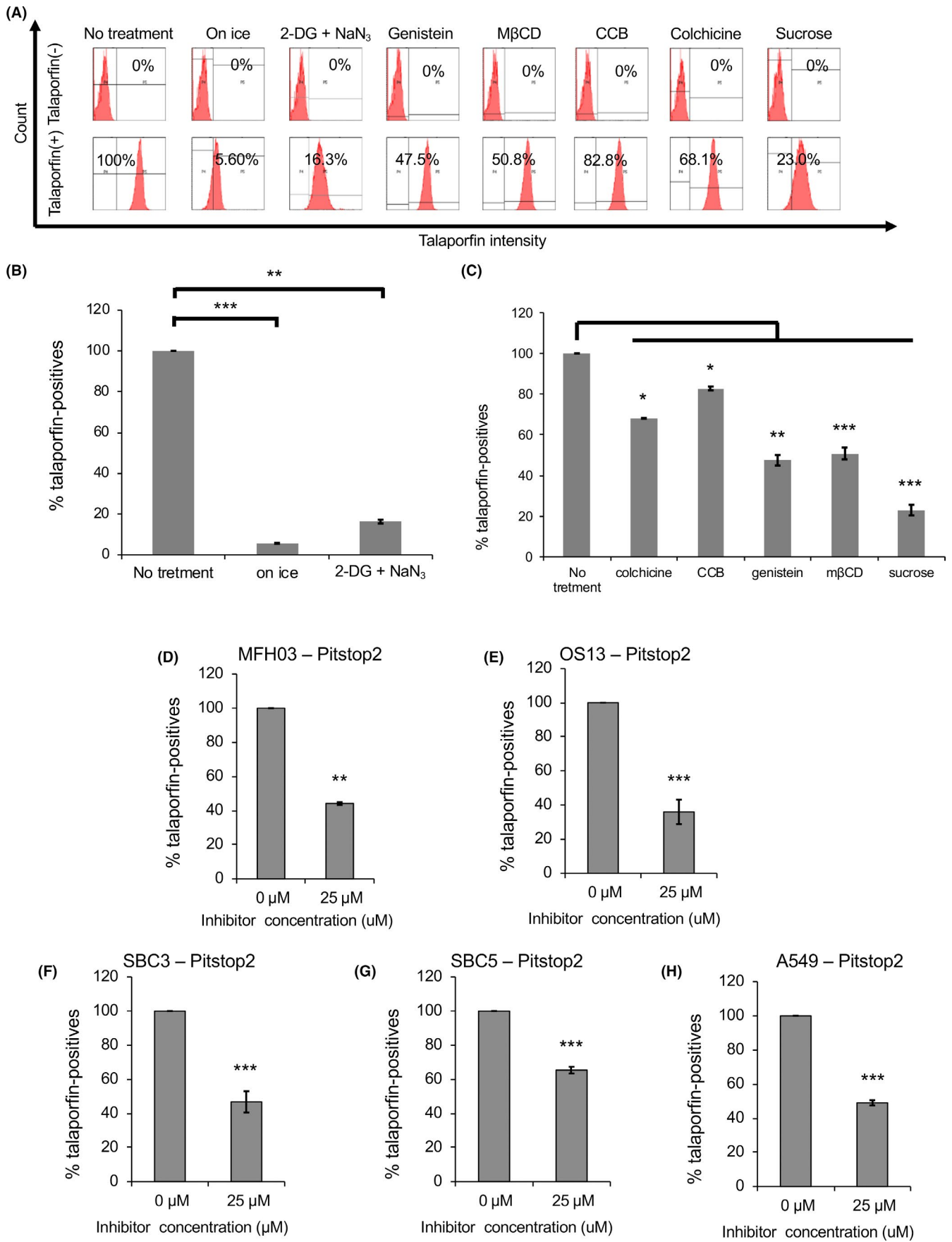


FIGURE 3 Uptake of talaporfin was suppressed by inhibition of endocytosis. (A) Fluorescence intensity of MFH03 with or without incubation with talaporfin previously treated with the indicated endocytosis inhibitors. The proportion of talaporfin-positive cells is indicated. Representative results of independent experiments ($n = 3$) are shown. (B, C) The proportion of talaporfin-positive cells of MFH03 with incubation with talaporfin previously treated with the indicated endocytosis inhibitors ($n = 3$). (D-H) Changes in talaporfin uptake after treatment with Pitstop2 ($n = 3$). Proportions of talaporfin-positive cells are shown. Data represent the means \pm SE. * $P < .05$, ** $P < .01$, *** $P < .005$

lung cancer and sarcoma cell lines. The colocalization of talaporfin consistent with Rab5a and LAMP1 was observed in the sarcoma cell line MFH03 and the lung cancer cell line SBC3 (Figure 2A, B). In contrast, talaporfin was not colocalized with mitochondria. Similar results were also observed in other lung cancer and sarcoma cell lines (Figure 2C-F). Intracellular talaporfin level increased with time (Figures S2-S7). These results suggested that talaporfin was transported from early endosomes to lysosomes.

3.3 | Talaporfin is taken up by endocytosis

We observed that the incorporated talaporfin accumulated in early endosomes and lysosomes. Therefore, we hypothesized that it might be taken into cancer cells by endocytosis. We analyzed changes in the uptake of talaporfin using endocytosis inhibitors (Figure 3A-C). Uptake was greatly reduced in MFH03 after incubation on ice. This observation suggested that talaporfin is taken into cells by active

transport. Moreover, the uptake of talaporfin was significantly reduced by culturing with 2-DG and NaN_3 , which inhibit intracellular ATP synthesis. This indicates that ATP is essential for talaporfin metabolism. In contrast to the high amounts of ATP produced by MFH03, the amounts produced in PBMC were very low (Figure S8). When the amount of intracellular ATP decreased, the amount of talaporfin uptake also decreased (Figure S9). Therefore, the uptake of talaporfin is dependent on the amount of intracellular ATP.

Sucrose, which is an inhibitor of clathrin-dependent endocytic lattice formation, also reduced talaporfin uptake. Genistein (an inhibitor of caveolae endocytosis), methyl- β -cyclodextrin (M β CD, an inhibitor of caveolae and lipid raft endocytosis), cytochalasin B (an inhibitor of phagocytosis and micropinocytosis), and colchicine (an inhibitor of microtubule formation) reduced the uptake of talaporfin. In contrast, chlorpromazine hydrochloride, which is an inhibitor of clathrin film formation, did not reduce uptake. Moreover, Pitstop2, which specifically inhibits clathrin-dependent endocytosis,¹⁴ significantly reduced the uptake of talaporfin in lung cancer and sarcoma

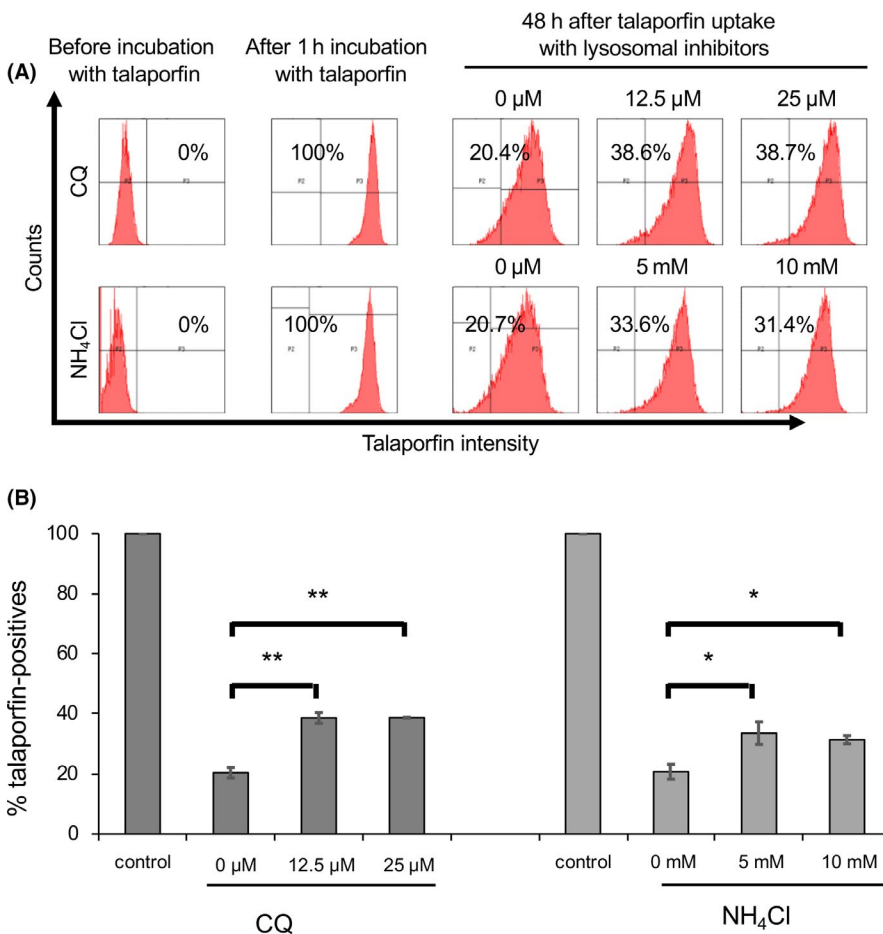
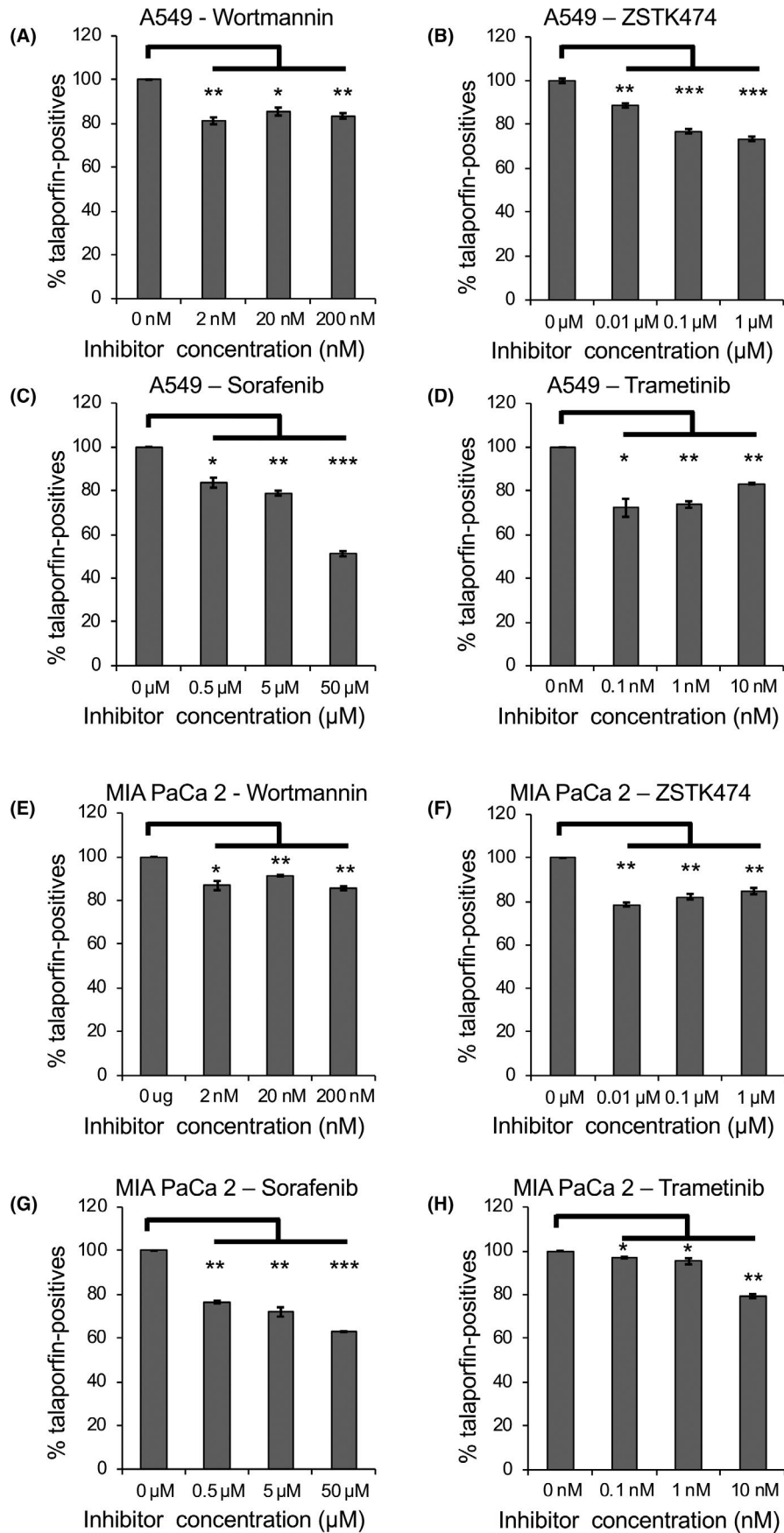


FIGURE 4 Elimination of talaporfin was suppressed by lysosomal inhibitors. (A) Fluorescence intensity of MFH03 with or without incubation with talaporfin previously treated with lysosomal enzyme inhibitors, chloroquine (CQ), and NH_4Cl at the indicated concentrations for 48 h. Proportions of the remaining talaporfin-positive cells are indicated. Representative results of independent experiments ($n = 3$) are shown. (B) Proportion of the remaining talaporfin-positive cells after lysosomal enzyme inhibitors ($n = 3$). Data represent the means \pm SE. * $P < .05$, ** $P < .01$



(Continues)

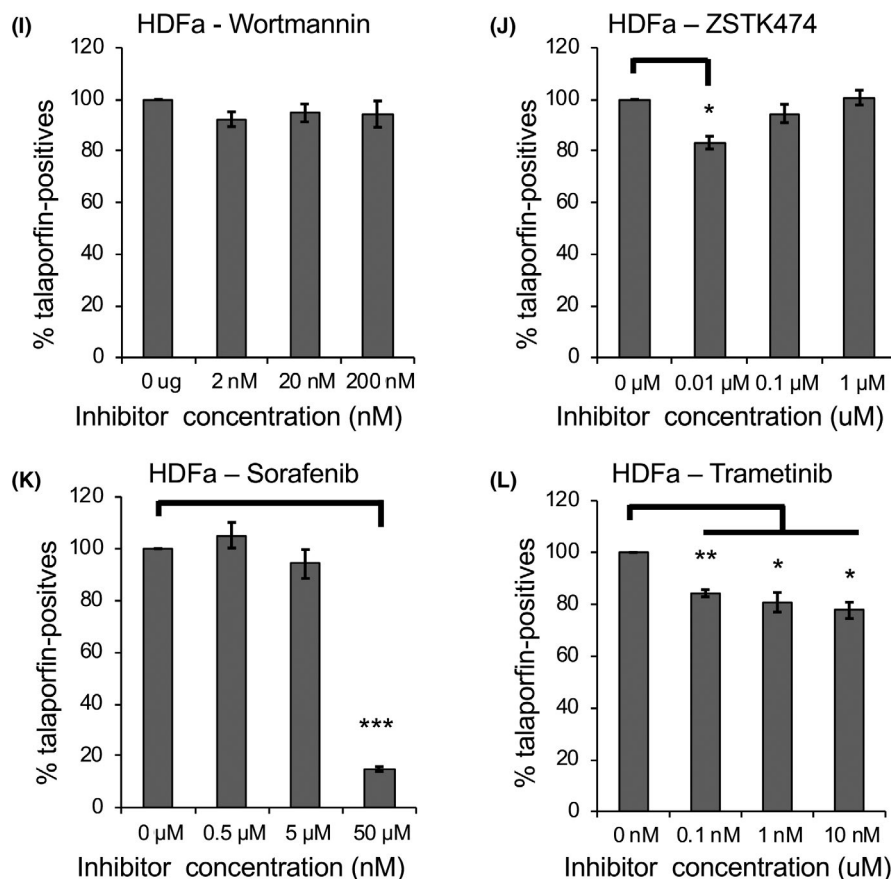


FIGURE 5 Inhibition of Ras signaling pathway suppresses the uptake of talaporfin in cancer cells with K-Ras mutation. Proportion of talaporfin-uptake cells treated with PI3K pathway inhibitors (wortmannin, ZSTK474) and MAPK pathway inhibitors (sorafenib, and trametinib) at the indicated concentrations in A549 (A-D), MIA Paca-2 (E-H), HDFa (I-L) ($n = 3$). HDFa was used as control without K-Ras mutation. Data represent the means \pm SE. * $P < .05$, ** $P < .01$, *** $P < .005$

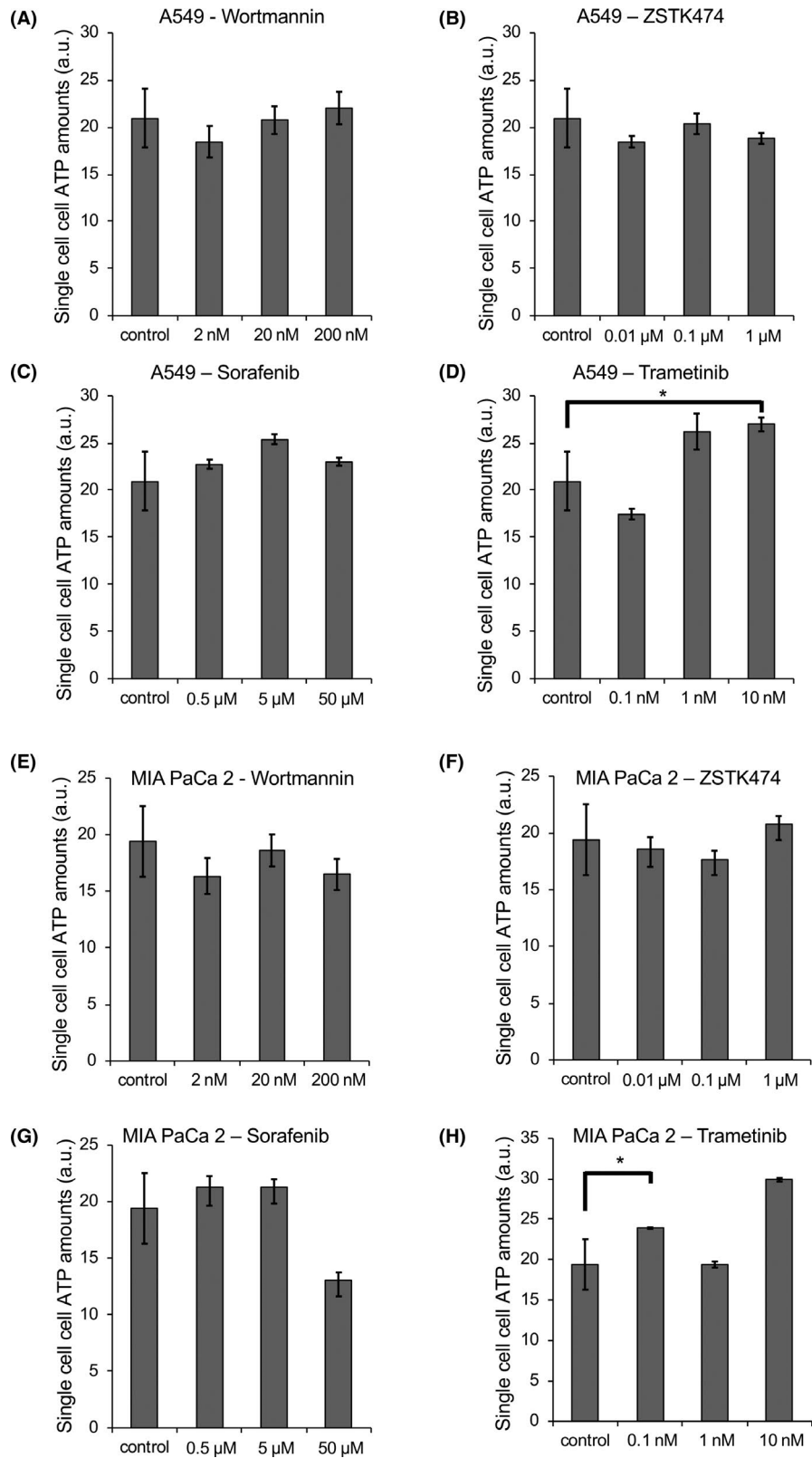
cell lines (Figure 3D-G). These results suggested that talaporfin is taken up via both endocytosis mechanisms, clathrin-dependent and caveolae endocytosis. In addition, macropinocytosis and phagocytosis are slightly involved. Microtubule formation also plays a role in the uptake of talaporfin.

3.4 | Intracellular disappearance pathway of talaporfin is by enzymatic degradation in lysosomes

Considering the colocalization of talaporfin with early endosomes and lysosomes, we hypothesized that the elimination of talaporfin is dependent on degradation by lysosomes. We analyzed MFH03 after treatment with the lysosomal degradation inhibitors chloroquine (CQ) or NH_4Cl , which suppressed lysosomal enzyme activity by increasing the internal pH of endosomes.¹⁵ Results showed that after culture with CQ or NH_4Cl for 48 hours, the decrease in fluorescence intensity of talaporfin was significantly inhibited (Figure 4A, B). These results suggested that enzymatic degradation in lysosomes contributed to the elimination of talaporfin in cancer cells.

3.5 | Talaporfin uptake is dependent on K-Ras activity

We observed that talaporfin was taken up by endocytosis, which required high ATP production. Talaporfin was then transferred to early endosomes and lysosomes, after which the lysosomal enzymes were degraded. However, Ras mutations might be involved in the activation of glycolysis and endocytosis.¹⁶⁻¹⁸ Therefore, we evaluated the changes in talaporfin uptake by the inhibition of the Ras signaling pathway in K-Ras mutant cancer cells, the lung cancer cell line A549, and the pancreatic cancer cell line MIA PaCa2 with K-Ras mutation.^{12,13} The human fibroblast cell line HDFa was used as a control. Wortmannin and ZSTK474 were used as inhibitors of PI3K, and sorafenib and trametinib were used as inhibitors of MAPK. Results showed that all inhibitors reduced talaporfin uptake in A549 and MIA PaCa2 cells (Figure 5A-H). In HDFa cells without K-Ras mutation, the inhibitory effects were slightly limited compared with A549 and MIA PaCa2 cells (Figure 5I-L). These results indicate that downstream of the K-Ras signaling pathway, both PI3K and MAPK pathways might promote the uptake of talaporfin. In contrast, A549 and MIA PaCa2 cells did not show any decrease in the amount of



(Continues)

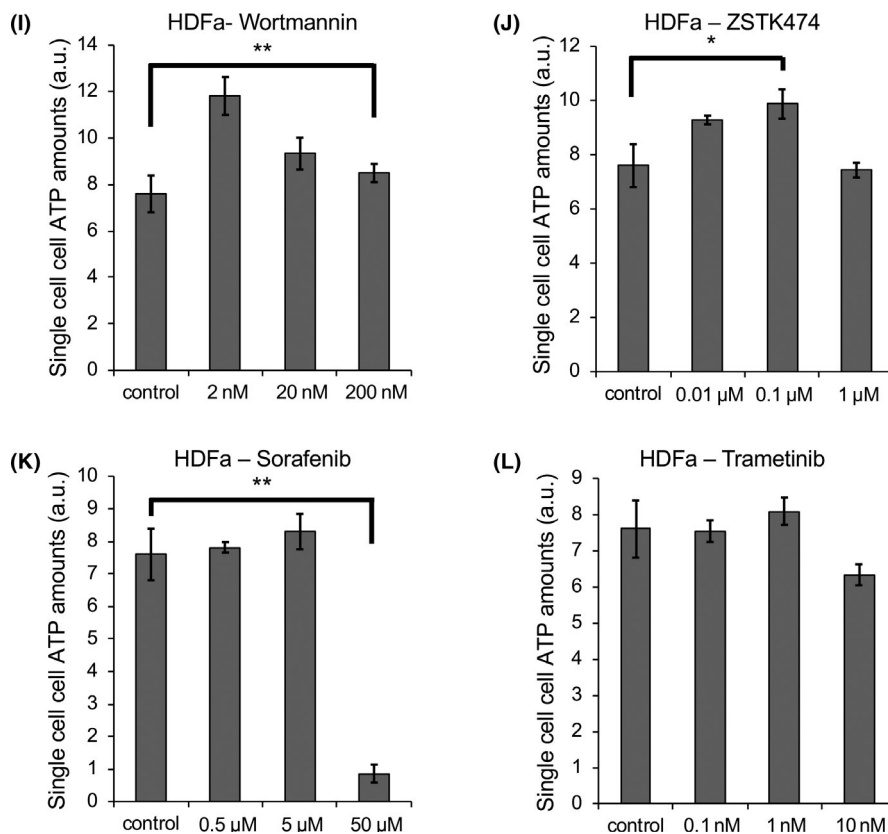


FIGURE 6 Inhibition of K-Ras did not decrease intracellular ATP. The amount of ATP in K-Ras mutated A549 (A-D) and MIA PaCa2 (E-H), and HDFa without mutation (I-L) after the treatment with K-Ras signaling pathway inhibitors are shown ($n = 3$). Single-cell ATP amounts were calculated using the following formula: single-cell ATP amounts = (total ATP amount)/(cell numbers). Data represent the means \pm SE. * $P < .05$, ** $P < .01$

ATP after treatment with all inhibitors (Figure 6A-H). HDFa, a normal keratinocyte cell line, showed a decrease in ATP production only after treatment with sorafenib at 50 $\mu\text{mol/L}$ (Figure 6I-L), which is similar to talaporfin uptake (Figure 5K). These results suggested that activation of the Ras signaling pathway could confer increased uptake of talaporfin but might be independent from intracellular ATP levels in cancer cells.

4 | DISCUSSION

In the present study, we analyzed the uptake and excretion of talaporfin in various carcinoma and sarcoma cell lines. Talaporfin was taken up by cancer cell lines, and the amount increased with time. This phenomenon is also observed in the clinical administration of talaporfin in cancer patients.¹⁹ In addition, a decrease of talaporfin over time was observed in all cancer cell lines.

In a previous report, the porphyrin compound Protoporphyrin IX was taken up and excreted by the ABC transporter.²⁰ Therefore, we first hypothesized that talaporfin was metabolized by ABC transporters. However, the transporters specifically expressed in cancer cell lines, in which the fluorescence intensity of talaporfin quickly decreased, could not be identified. Instead, we showed that talaporfin

was taken up by endocytosis, translocated from early endosomes to lysosomes, and degraded by lysosomal enzymes in cancer cell lines. These results are consistent with previous reports showing that talaporfin accumulates in lysosomes.⁸

The combination of 2-DG and NaN_3 inhibited the uptake of talaporfin mediated by the suppression of ATP production. Ice treatment also inhibited the uptake of talaporfin. These results suggested that the uptake mechanism of talaporfin is dependent on active transport including endocytosis. Sucrose and Pitstop2 are inhibitors of clathrin-dependent endocytosis, and genistein is an inhibitor of caveolae-dependent endocytosis. Treatment with these inhibitors also reduced the uptake of talaporfin. These results suggested that uptake might be dependent on both clathrin-dependent and caveolae-dependent endocytosis. We examined the pathway of talaporfin elimination in cancer cells using inhibitors of lysosomal enzyme, CQ and NH_4Cl , which inhibit degradative activity through the increase of pH in the lysosome. After treatment with CQ and NH_4Cl , intense uptake of talaporfin was maintained for 24 hours. From the observations described above, we considered that uptake of talaporfin might be eliminated in cancer cells by enzymatic degradation by lysosomes.

Talaporfin was taken up by endocytosis over time in various cancer cell lines but not in PBMC. In clinical settings, photosensitizers such as talaporfin are also selectively taken up into cancer cells.¹

Generally, endocytosis is the ubiquitous machinery maintained not only in cancer cells but also in normal cells.⁵ It is not yet clear why talaporfin is not taken up by normal cells, including PBMC. In the present study, we observed that the intracellular amount of ATP is far higher in cancer cell lines than in PBMC. In addition, ATP is required for the uptake of talaporfin in cancer cell lines. This might be a possible reason for the non-uptake of talaporfin in PBMC. Talaporfin is taken up via endocytosis, which is a generally conserved phenomenon among both normal and transformed malignant cells. Therefore, talaporfin uptake might not be specific to malignant cells but could be strongly increased in them. In cancer cells, constitutive upregulation and activation of dynamin-1 might contribute to clathrin-dependent endocytosis, which alters signaling to enhance survival, migration, and proliferation.²¹ Mutant forms of p53 and Ras might also harness endocytosis in cancer cells.⁶ Therefore, upregulated endocytosis, which is an active transporter, might depend on high amounts of intracellular ATP.

Moreover, in cancer cell lines with K-Ras mutations, the uptake of talaporfin was suppressed by PI3K and MAPK inhibitors. This might indicate that the mutation of K-Ras promotes the uptake of talaporfin. Fujioka et al reported that the Ras-PI3K signaling pathway is involved in the regulation of clathrin-independent endocytosis.¹⁶ Roy et al showed that K-Ras mutations regulate caveolae-dependent endocytosis in human colon cancer.¹⁷ These studies suggest that activation of the Ras signaling pathway might promote caveolae-dependent endocytosis more than clathrin-dependent endocytosis. It has also been reported that mutation of K-Ras enhances the glycolytic pathway by a glucose transporter.^{18,22} These studies suggest that the promotion of talaporfin uptake via mutated K-Ras activation is mediated by the high amount of intracellular ATP. Therefore, we investigated whether inhibition of K-Ras reduced the amount of intracellular ATP. However, the amount of ATP was maintained by PI3K and MAPK inhibitors in cancer cell lines. These results support the idea that activation of K-Ras signaling could promote the uptake of talaporfin, but this might be independent of the amount of intracellular ATP.

Cell death after PDT could induce anti-tumor immune responses by activation of immune cells, cytokine release, CD8+ T cell infiltration, and the formation of immunological memory,^{3,4} which suggests possible benefits of combination therapy using PDT and immunotherapy.

In conclusion, we found that uptake of talaporfin was mediated by both clathrin-dependent and caveolae-dependent endocytosis in carcinoma and sarcoma cells; talaporfin was then translocated from early endosomes to lysosomes and was finally degraded by lysosomal enzymes. We also demonstrated that ATP is essential for the uptake of talaporfin, and that the activation of K-Ras is involved as a regulatory mechanism. These results provide new insights into the metabolism of talaporfin in cancer cells for the enhancement of PDT for carcinoma and sarcoma.

ACKNOWLEDGMENTS

The authors thank Ms Asuka Akamatsu, Ms Chisa Fuchizaki, Ms Aiko Murai, Ms Junko Yanagawa, Ms Kazue Watanabe and Ms Eri Saka for

their technical assistance. This work was supported by grants from JSPS KAKENHI (25462344 and 20H03807 to T. Tsukahara, 17H01540 to T. Torigoe), the Takeda Science Foundation (2018-Kenkyu-Shorei Keizoku to T. Tsukahara) and the Research Grant of Princess Takamatsu Cancer Research Fund (19-25125 to T. Tsukahara).

CONFLICTS OF INTEREST

The authors declare no conflicts of interest.

ORCID

Tomohide Tsukahara  <https://orcid.org/0000-0002-3678-4359>

Terufumi Kubo  <https://orcid.org/0000-0001-9274-2551>

Yoshihiko Hirohashi  <https://orcid.org/0000-0002-0608-3914>

REFERENCES

- Prazmo EJ, Kwasny M, Lapinski M, Mielczarek A. Photodynamic therapy as a promising method used in the treatment of oral diseases. *Adv Clin Exp Med*. 2016;25:799-807.
- Awasthi K, Yamamoto K, Furuya K, Nakabayashi T, Li L, Ohta N. Fluorescence characteristics and lifetime images of photosensitizers of talaporfin sodium and sodium pheophorbide a in normal and cancer cells. *Sensors (Basel)*. 2015;15:11417-11430.
- Hou X, Tao Y, Pang Y, Li X, Jiang G, Liu Y. Nanoparticle-based photothermal and photodynamic immunotherapy for tumor treatment. *Int J Cancer*. 2018;143:3050-3060.
- Kabingu E, Vaughan L, Owczarczak B, Ramsey KD, Gollnick SO. CD8+ T cell-mediated control of distant tumours following local photodynamic therapy is independent of CD4+ T cells and dependent on natural killer cells. *Br J Cancer*. 2007;96:1839-1848.
- Hinze C, Boucrot E. Endocytosis in proliferating, quiescent and terminally differentiated cells. *J Cell Sci*. 2018;131(23):jcs216804.
- Mellman I, Yarden Y. Endocytosis and cancer. *Cold Spring Harb Perspect Biol*. 2013;5:a016949.
- Pasello M, Giudice AM, Scotlandi K. The ABC subfamily A transporters: Multifaceted players with incipient potentialities in cancer. *Semin Cancer Biol*. 2020;60:57-71.
- Kessel D, Andrzejak M, Santiago M. Effects of endosomal photodamage on membrane recycling and endocytosis. *Photochem Photobiol*. 2011;87:699-706.
- Nabeta Y, Kawaguchi S, Sahara H, et al. Recognition by cellular and humoral autologous immunity in a human osteosarcoma cell line. *J Orthop Sci*. 2003;8:554-559.
- Tsukahara T, Kawaguchi S, Ida K, et al. HLA-restricted specific tumor cytotoxicity by autologous T-lymphocytes infiltrating metastatic bone malignant fibrous histiocytoma of lymph node. *J Orthop Res*. 2006;24:94-101.
- Mizushima E, Tsukahara T, Emori M, et al. Osteosarcoma-initiating cells have metabolic features of high aerobic glycolysis and attenuation of OXPHOS mediated by LIN28B. *Cancer Sci*. 2020; 111:36-46. <https://doi.org/10.1111/cas.14229>
- Minchom A, Thavasu P, Ahmad Z, et al. A study of PD-L1 expression in KRAS mutant non-small cell lung cancer cell lines exposed to relevant targeted treatments. *PLoS One*. 2017;12:e0186106.
- Brauswetter D, Gurbi B, Varga A, et al. Molecular subtype specific efficacy of MEK inhibitors in pancreatic cancers. *PLoS One*. 2017;12:e0185687.
- von Kleist L, Stahlschmidt W, Bulut H, et al. Role of the clathrin terminal domain in regulating coated pit dynamics revealed by small molecule inhibition. *Cell*. 2011;146:471-484.
- Misinzio G, Delputte PL, Nauwynck HJ. Inhibition of endosome-lysosome system acidification enhances porcine circovirus 2 infection of porcine epithelial cells. *J Virol*. 2008;82:1128-1135.

16. Fujioka Y, Tsuda M, Hattori T, et al. The Ras-PI3K signaling pathway is involved in clathrin-independent endocytosis and the internalization of influenza viruses. *PLoS One*. 2011;6:e16324.
17. Roy UK, Rial NS, Kachel KL, Gerner EW. Activated K-RAS increases polyamine uptake in human colon cancer cells through modulation of caveolar endocytosis. *Mol Carcinog*. 2008;47:538-553.
18. Gaglio D, Metallo CM, Gameiro PA, et al. Oncogenic K-Ras decouples glucose and glutamine metabolism to support cancer cell growth. *Mol Syst Biol*. 2011;7:523.
19. Akimoto J, Fukami S, Ichikawa M, Mohamed A, Kohno M. Intraoperative photodiagnosis for malignant glioma using photosensitizer talaporfin sodium. *Front Surg*. 2019;6:12.
20. Kawai N, Hirohashi Y, Ebihara Y, et al. ABCG2 expression is related to low 5-ALA photodynamic diagnosis (PDD) efficacy and cancer stem cell phenotype, and suppression of ABCG2 improves the efficacy of PDD. *PLoS One*. 2019;14:e0216503.
21. Schmid SL. Reciprocal regulation of signaling and endocytosis: Implications for the evolving cancer cell. *J Cell Biol*. 2017;216:2623-2632.
22. Ying H, Kimmelman AC, Lyssiotis CA, et al. Oncogenic Kras maintains pancreatic tumors through regulation of anabolic glucose metabolism. *Cell*. 2012;149:656-670.

SUPPORTING INFORMATION

Additional supporting information may be found online in the Supporting Information section.

How to cite this article: Saito T, Tsukahara T, Suzuki T, et al. Spatiotemporal metabolic dynamics of the photosensitizer talaporfin sodium in carcinoma and sarcoma. *Cancer Sci*. 2021;112:550-562. <https://doi.org/10.1111/cas.14735>